Two-Dimensional (2D) ATR−FTIR Spectroscopic Study on Water Diffusion in Cured Epoxy Resins

Mojun Liu, Peiyi Wu,* Yifu Ding, Gang Chen, and Shanjun Li*,†

Department of Macromolecular Science and The Key Laboratory of Polymer Engineering Science, Fudan University, Shanghai, 200433, China

Received October 19, 2001

ABSTRACT: A novel experimental approach, based on time-resolved two-dimensional (2D) ATR−FTIR spectroscopy has been used to study water diffusion behavior of novolac epoxy resins cured with novolac resin and novolac acetate resin named as EP and EPA, respectively. The diffusion coefficients calculated by a nonlinear curve fitting are quite consistent with the results of gravimetric analysis. In 2D-IR spectra, the splitting of the water OH vibration band at 2800−3700 and 1500−1800 cm^{-1} shows that there are two different states of water in epoxy networks, in which one could be confined into free volume (microvoids) or molecularly dispersed with less hydrogen-bonding (bulk dissolved), while the other could be attributed to bound water forming strong hydrogen-bonding with hydrophilic groups of epoxy networks. The sequential order of intensity changes of the two water bands elucidates that, in the process of water diffusion into epoxy networks, water molecules first bind with specific hydrophilic groups as bound water and then diffuse into free volume (microvoids) or molecularly dispersed with less hydrogen-bonding (bulk dissolved). The wavenumber difference of OH vibration band appearing from bound water between EP and EPA indicates that water molecules form much stronger hydrogen-bonding with EP networks than with EPA networks.

1. Introduction

The behavior of water diffusion in epoxy networks has raised a great scientific interest over the past 40 years[1−6] because water sorption would brought about a deterioration in excellent properties of epoxy resins and had become a very serious drawback in application of epoxy materials. Several sorption models had been established about the state of water molecules in epoxy networks. One presumed water to be diffused into free volume,[7−10] the other[11] was the interaction concept that water molecules coupled strongly with certain hydrophilic groups such as hydroxyl or amine to form hydrogen-bonding in epoxy resins. Woo and Piggott[12] suggested clustering of water molecules in epoxy resins. Adamson[13] concluded that some water molecules interacted by forming hydrogen bonds with hydrophilic groups in epoxy resins, while the other water molecules were retained in free volume. Zhou[3] found that there were two types of water in epoxy resins in which one disrupted the interchain interaction, resulting in increasing segment mobility of bulk, the other formed multiple hydrogen bonds with epoxy networks, resulting in secondary cross-linking. Apicella et al.[14] proposed that there were three sorption models in glassy epoxy:

(1) Bulk dissolution of water in glassy epoxy networks.

(2) Moisture sorption onto the surface of excess free volume.

(3) Hydrogen-bonding between water and polymer hydrophilic groups.

Moy[15] reported that water molecules in lower concentration bind with specific chain segments or groups, but as the water vapor concentration increased, multilayer sorption water molecules existed as free water. Substantial disagreement still persisted among these models, No single theory or model existed with sufficient experimental support to explain all sorption phenomena. In our group, much work[16,17] has been perfomed on contributions of nanopores (microvoids), side group polarities, and side group flexibilities for water diffusion behavior as well as the effects of water sorption on mechanical relaxation behavior in novolac epoxy networks.

There have been a number of papers published on the diffusion of water into polymer interface using vibrational spectroscopy.[18−21] Changes of frequency, intensity, and shapes of water bands have been in terms of bound and free water, water clustering, water orientation, and water networking. As a technique sensitive to the interaction between the water and polymer, ATR−FTIR spectra have been quickly developed for studying the water diffusion behavior of polymer systems.[22−25] As Marechal[24] has pointed out, the spectra obtained are free from saturation artifacts, and the sampling depth is dependent on controllable parameters and is on the order of 0.5−2.0 μm. The spectra can be collected in real time on the scale of the diffusion process at a polymer interface in contact with ATR crystal.

Generalized two-dimensional (2D) IR spectroscopy proposed by Noda[26−29] has received great attention in recent years. It emphasizes spectral features not readily observable in conventional one-dimensional (1D) spectra and also probes the specific order of certain events taking place with the development of a controlling physical variable. Many applications of 2D correlation spectroscopy have been reported[30−34] such as temperature-dependent spectral variations, concentration-dependent spectral changes, and time-dependent spectral changes.

In this article, we monitor the water diffusion process in novolac epoxy resins cured with phenol novolac resin and phenol novolac acetate resin named EP and EPA, respectively, by time-resolved ATR−FTIR spectrometry. Using a 2D correlation analysis, the original wide water OH bands in 1D-IR spectra can be effectively differenti-

* Corresponding authors. Fax: 0086-21-65640293.
† E-mail: sjli@fudan.edu.cn.

10.1021/ma011819f CCC: $22.00
Published on Web 06/04/2002

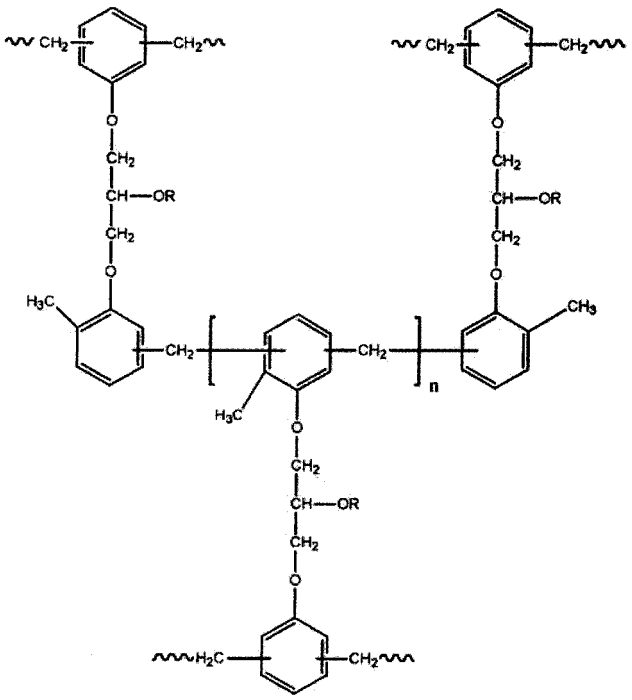

Figure 1. Chemical structures of EP and EPA. For ZP R = H, for ZPA R = CH_3CO.

ated as two bands, and their band positions and relative variation rates are determined. The behavior of water diffusion of the two systems is also discussed.

2. Experimental Section

2.1. Materials. *o*-Cresol (2-methylphenol) novolac epoxy resin (YDCN-702p from Tohto Kasei, epoxy equivalent: 200 ~ 230 g equiv^{-1}) and Novolac (H-1, from Sumitomo, hydroxyl equivalent: 107 g equiv^{-1}) were used in this work. The esterified curing agents were synthesized from novolac (NOV) and acetic anhydride according to the procedure reported previously,[16] 2-Methylimidazole (2MI, from Wuhan Pharmaceutical Co.) was used as curing accelerator.

2.2. Film Preparation. The epoxy resins were cured by the curing agents according to the stoichiometric ratios with 0.5% of 2-MI. The fresh mixture of the raw materials was dissolved in A. R. acetone. Then the solution was cast onto a 75 mm × 25 mm × 1 mm microscope slide. After being left in the air at room temperature on a metal plate for 1 day, the resins was cured in a vacuum oven at 45 °C/15 min, 80 °C/15 min, 120 °C/3 h, 150 °C/2 h, and 180 °C/2 h and finally cooled slowly down to room temperature. Then the films were peeled off for use. The thickness of the sample films was measured by a Coatest-1000 nonferrous digital coating thickness gauge. The chemical structures of the cured resins EP and EPA are shown in Figure 1.

2.3. Diffusion Measurements by Time-Resolved ATR−FTIR. All time-resolved ATR−FTIR measurements were performed at 24 °C using a Nicolet Nexus Smart ARK FTIR spectrometer equipped with a DTGS−KBr detector, solid cell accessories, and a ZnSe IRE crystal. The spectra were measured at 4 cm^{-1} resolution and eight scans; the wavenumber range was 650−4000 cm^{-1}. The film-covered IRE crystal with a filter paper above the sample film was mounted in an ATR cell, and the spectra of the dry film was collected as background spectra; then without moving the sample, distilled water was injected into the filter paper while starting the data acquisition by a macro program. A typical sorption loop lasted about 15 min. For EP, the acquisition time interval was 33 s; for EPA, the acquisition time interval was 27 s. The time-resolved ATR−FTIR spectra in two wavenumber ranges of sorbed water in EP and EPA were obtained from subtraction spectra of the background and the wet sample films (in Figure 2 and Figure 3).

2.4. Two-Dimensional Correlation Analysis. Six spectra at equal time intervals in certain wavenumber range were selected to 2D correlation analysis using the software "2D Pocha" which was composed by Daisuke Adachi (Kwansei Gakuin University). The time-averaged 1D reference spectrum is shown at the side and top of the 2D correlation maps for comparison. In the 2D correlation maps, unshaded regions indicate positive correlation intensities, while shaded regions indicate negative correlation intensities.

3. Results and Discussion

3.1. Diffusion Characterastics from Time-Resolved ATR−FTIR Spectra. As shown in Figure 2A and Figure 3A, the IR spectra of sorbed water in the range of 2700−3900 cm^{-1} reveal an increasing intensity of OH variation band (located at 3200−3800 cm^{-1}) as water diffusing into epoxy networks. Equation 1[23] is given to calculate diffusion coefficient from ATR−FTIR spectra.

$$\frac{A_t}{A_\infty} = 1 - \frac{8\gamma}{\pi[1-\exp(2L\gamma)]}\sum_{n=0}^{\infty}\left[\frac{\exp\left(\frac{-D(2n+1)^2\pi^2 t}{4L^2}\right)\left[\frac{(2n+1)\pi}{2L}\exp(-\gamma 2L) + (-1)^n(2\gamma)\right]}{(2n+1)\left(4\gamma^2 + \left(\frac{(2n+1)\pi^2}{2L}\right)^2\right)}\right] \quad (1)$$

In this expression, A_t is band absorbance of ATR−FIIR spectra at time t, A_∞ is the equilibrium band absorbance, and the penetration depth of the evanescent wave γ can be defined from eq 2.[35]

$$\gamma = \lambda_1/2\pi(\sin^2\theta - {n_{21}}^2) \quad (2)$$

λ_1 is the wavelength of the infrared beam in the ATR element, θ is the incidence angle of radiation at the polymer/element interface, and n_{21} is the ratio of the refractive index of polymer to that of the element. The diffusion coefficient was calculated by a nonlinear curve fitting to eq 1 from integral of OH stretching variation band area vs time. Four parameters, a, d, m, and l were defined as following: a was the zero correction parameter, d was the diffusion coefficient, m was the equilibrium water uptake, and l was the film thickness (invariable). The fitting curves and analysis results of EP and EPA were shown in Figure 4 and Table 1, respectively.

The fitting results show that equilibrium water uptake of EPA is much lower than that of EP, while diffusion coefficient of EPA is much higher. This is consistent with the result of gravimetric analysis reported in our previous work[16] (in Table 2). It was explained that the affinity of water molecules to the resin hydrophilic groups which was controlled by polarity of these groups can increase the water uptake, but it could also retard the diffusion of water. Furthermore, during a sorption process, a glassy polymer had to adjust its polymer segments to adapt to the diffusion of water, which was related to the flexibility of the side group. Therefore, the better the flexibility of the side group was, the higher the diffusion coefficient was, while the better the polarity of the side groups was, the lower

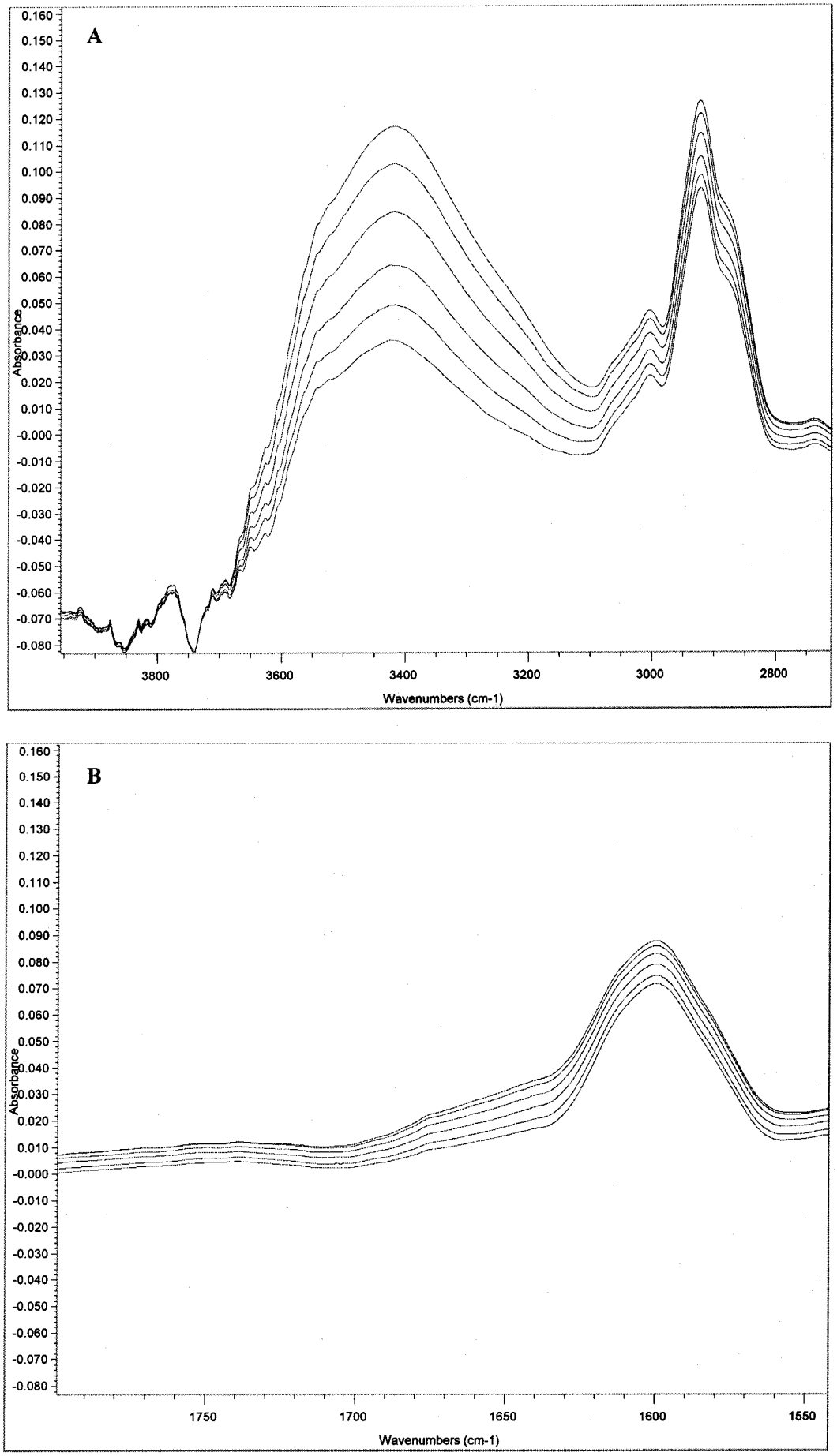

Figure 2. ATR−FTIR spectra of sorbed water in EP: (A) at 2700−3900 cm^{-1}; (B) at 1540−1800 cm^{-1}.

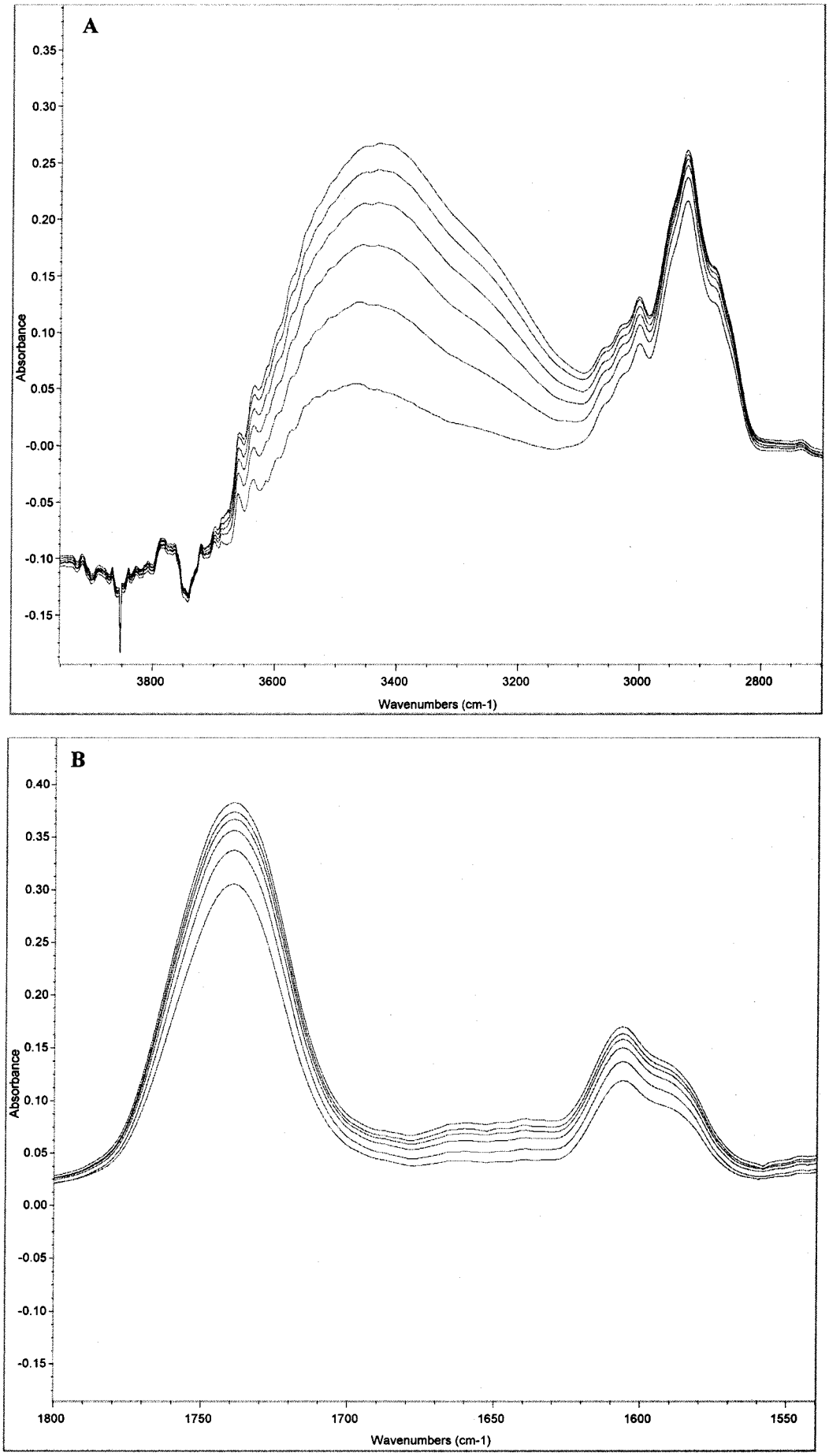

Figure 3. ATR−FTIR spectra of sorbed water in EPA: (A) at 2700−3900 cm^{-1}; (B) at 1540−1800 cm^{-1}.

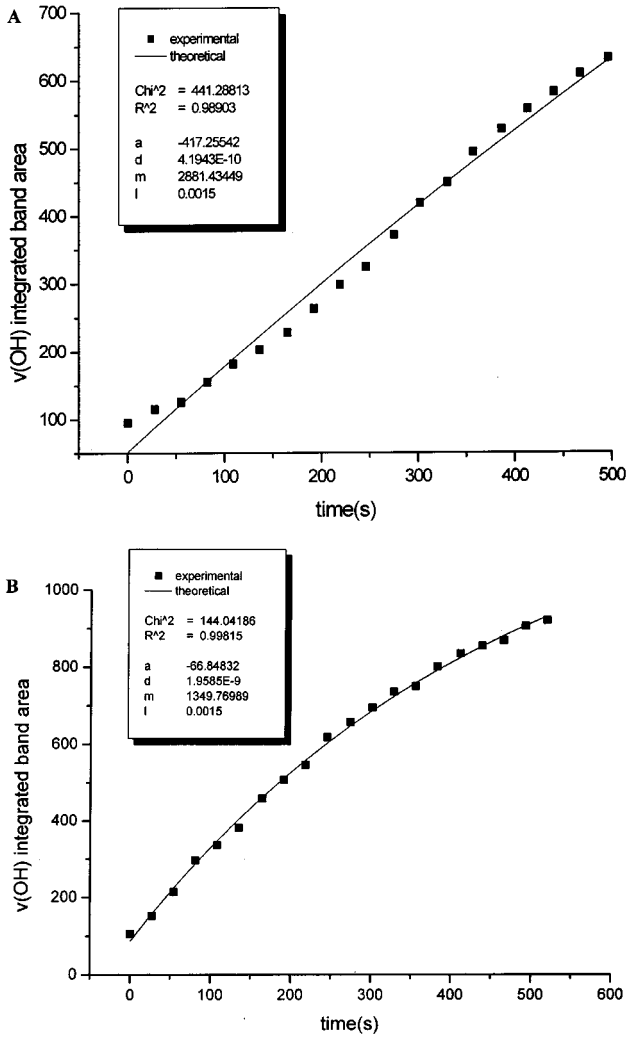

Figure 4. Fitting curves of sorbed water in EP and EPA: (A) EP; (B) EPA.

Table 1. Fitting Results from ATR−FTIR Spectra

	EP	EPA
a^a	−417	−67
m^a	2881	1350
l (cm)	0.0015	0.0015
d (10^{-9} cm^2 s^{-1})	0.42	1.96

[a] Zero correction parameter a and equilibrium water uptake m are variable parameters; their units are the integrals of the band area.

Table 2. Diffusion Results from Gravimetric Measurement and ATR−FTIR Fitting

	gravimetric results		IR fitting result	
	equilib water uptake	diffusion coeff (10^{-9} cm^2 s^{-1})	equilib water uptake[a]	diffusion coeff (10^{-9} cm^2 s^{-1})
EP	2.13%	2.4	2881	0.4
EPA	0.77%	9.5	1350	1.9

[a] The unit of equilibrium water uptake is the integral of the band area.

the diffusion coefficient was. Therefore, the diffusion coefficient of EPA is higher than that of EP because the polarity of hydroxyl groups in EP networks is much higher than that of carboxyl groups in EPA networks, while the side group flexibility of EP is not better than that of EPA.

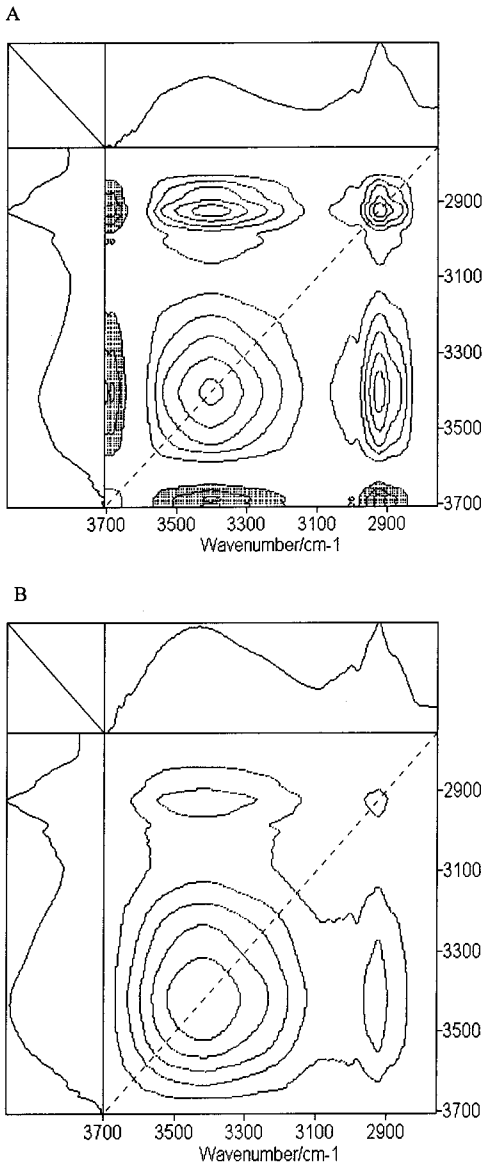

Figure 5. Synchronous 2D correlation spectra at 2800−3700 cm^{-1}: (A) EP; (B) EPA.

3.2. Two-Dimensional Correlation Analysis. 3.2.1. The Range 2800−3700 cm^{-1}. The synchronous correlation spectra of EP and EPA in the range 2800−3700 cm^{-1} were shown in Figure 5.

More information can be obtained from the corresponding asynchronous correlation spectra of EP and EPA in Figure 6. Asynchronous cross-peak $\psi(\upsilon_1,\upsilon_2)$ indicates that the bands υ_1 and υ_2 vary out of phase with each other, and the absence of Asynchronous cross-peak $\psi(\upsilon_1,\upsilon_2)$ suggests that the bands υ_1 and υ_2 change synchronously. The wide water vibration band at 3200−3600 cm^{-1} is split into two separate bands υ_1 and υ_2 located around 3396 and 3129 cm^{-1} in EP and around 3480 and 3249 cm^{-1} in EPA, which overlap in the 1D-IR spectra. It suggests that there are two different states of water in epoxy networks. If the water molecules form hydrogen bonds, the water OH stretching vibration band will shift to a lower wavenumber compared with the that of free water; thus, in these two water bands, one at higher wavenumber could be water molecules distributed into free volume (microvoids) or molecularly dispersed with less hydrogen-bonding (bulk dissolved), while the other at lower wavenumber reveal-

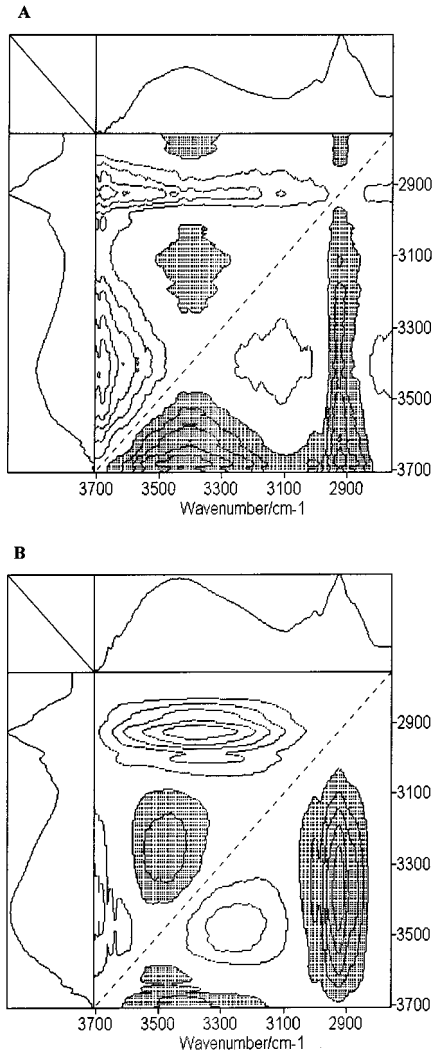

Figure 6. Asynchronous 2D correlation spectra at 2800−3700 cm^{-1}: (A) EP; (B) EPA.

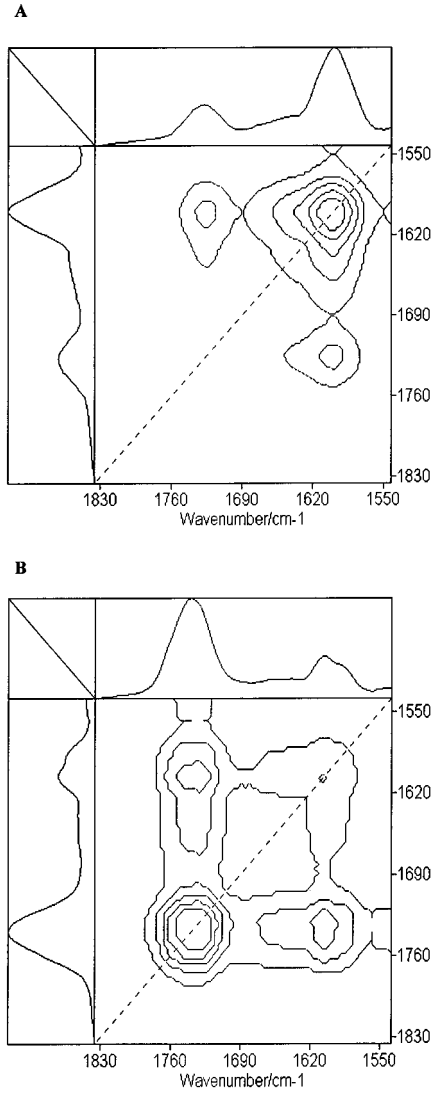

Figure 7. Synchronous 2D correlation spectra at 1500−1800 cm^{-1}: (A) EP; (B) EPA.

ing the strong hydrogen-bonding interactions between hydrophilic groups of epoxy networks and water molecules is attributed to bound water. The OH band appearing from bound water in EP at 3129 cm^{-1} has a considerably lower wavenumber than that in EPA at 3249 cm^{-1}, indicating that water molecules form stronger hydrogen-bonding with EP networks than with EPA networks, because the hydrogen-bonding between water molecules and carboxyl groups in EPA is not as strong as that between water molecules and hydroxyl groups in EP; in addition, hydrophobic groups CH_3 near carboxyl groups in EPA encumber water molecules binding with carboxyl groups.

The sign of asynchronous correlation peak $\psi(\upsilon_1,\upsilon_2)$ gives information about the sequential order of intensity changes between band υ_1 and band υ_2. According to the publications of Noda,[26] if $\Phi(\upsilon_1,\upsilon_2) > 0$, $\psi(\upsilon_1,\upsilon_2)$ is positive (unshaded area), band υ_1 will vary prior to band υ_2, and if $\psi(\upsilon_1,\upsilon_2)$ is negative (shaded area), band υ_1 will vary behind band υ_2. In Figure 6A, ψ(3396,3129) is negative, suggesting that the band at 3129 cm^{-1} varies prior to the band at 3396 cm^{-1}; it means in EP networks that the bound water (forming strong hydrogen-bonding with epoxy networks) is produced prior to the water diffused into free volume (microvoids) or water molecularly dispersed with less hydrogen-bonding (bulk water). The same result for EPA is obtained from Figure 6B. It is concluded that in the process of water diffusion into epoxy networks, water molecules first bind with specific hydrophilic groups as bound water and then diffuse into free volume (microvoids) or are molecularly dispersed with less hydrogen-bonding (bulk dissolved).

3.2.2. The Range 1500−1800 cm^{-1}. The synchronous correlation spectra of EP and EPA in the range 1500−1800 cm^{-1} were shown in Figure 7. In the 1D reference spectra of Figure 7B at the top and side of the 2D correlation maps, two main bands appearing in the ranges 1700−1780 and 1550−1680 cm^{-1} are respectively assigned to bulk CO vibration and water OH bending vibration. During water diffusion, epoxy networks adjust their segments to adapt water diffusion, causing relaxation of material; therefore, the carboxyl band variation near 1750 cm^{-1} could be attributed to interaction between water molecules and epoxy carboxyl groups.

The corresponding asynchronous correlation spectra of EP and EPA in the range 1500−1800 cm^{-1} (in Figure 8) show that the water bending vibration band around 1600−1650 cm^{-1} is also split into two separate bands (υ_1,υ_2) located around 1666 and 1600 cm^{-1} in EP and around 1654 and 1604 cm^{-1} in EPA. It also suggested that there existed two different states of water in epoxy

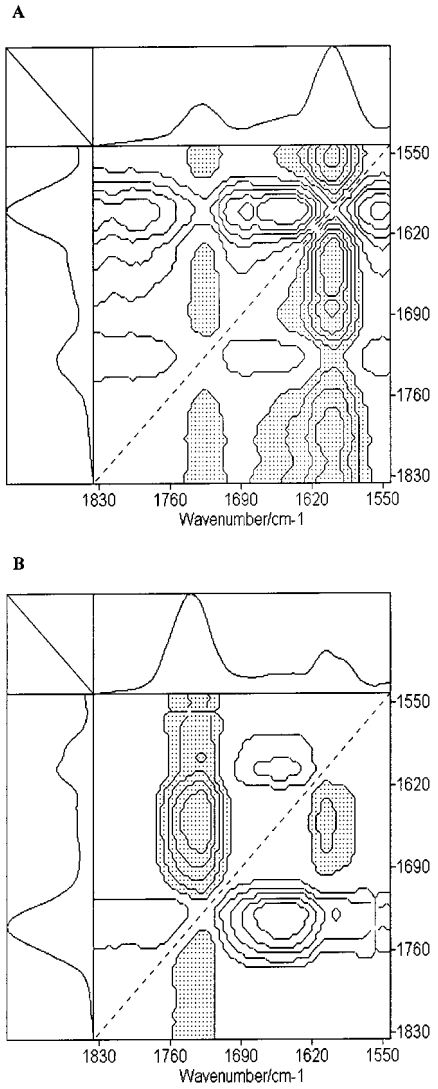

Figure 8. Asynchronous 2D correlation spectra at 1500−1800 cm^{-1}: (A) EP; (B) EPA.

networks: distributed in excess free volume (microvoids) or molecularly dispersed with less hydrogen-bonding (bulk dissolved), forming stronger hydrogen-bonding interactions between hydrophilic groups of epoxy and water molecules as bound water. The former water locates at a lower wavenumber, the latter locates at a higher wavenumber because the water bending vibration band would shift to a higher wavenumber compared with that of free water if the water molecules form hydrogen bonds. Similarly, the OH band of EP at 1666 cm^{-1} appearing from bound water has an obviously higher wavenumber than that of EPA at 1654 cm^{-1}, indicating that water molecules form stronger hydrogen bonds with EP networks than with EPA networks.

Additionally, the sign of the asynchronous correlation peak $\psi(\upsilon_1,\upsilon_2)$ given information about the sequential order of two water states is quite consistent with the results of the range 2800−3700 cm^{-1} as discussed in section 3.2.1.

4. Conclusion

A time-resolved 2D ATR−FTIR technique has been used to study water diffusion behavior in epoxy resins EP and EPA. The issues about diffusion kinetics, water state existing in epoxy networks and water−polymer interactions are discussed.

1. By a nonlinear curve fitting to Fickian diffusion equation, the diffusion coefficients of EP and EPA are calculated, which are consistent with gravimetric results reported in our previous works, diffusion coefficient of EPA is quite higher than that of EP.

2. The splitting of the water variation band in two ranges of 2D-IR spectra elucidates that there exist two states of water in epoxy networks, in which one could be confined into free volume (microvoids) or molecularly dispersed with less hydrogen-bonding (bulk dissolved); the other could be attributed to bound water forming strong hydrogen-bonding interactions with hydrophilic groups of epoxy networks. Furthermore, in the process of water diffusion into epoxy networks, water molecules first bind with specific hydrophilic groups as bound water and then diffuse into free volume (microvoids) or bulk dissolved.

3. The wavenumber difference of OH variation band appearing from the bound water between EP and EPA means that water molecules form much stronger hydrogen bonds with EP networks than that with EPA networks.

Acknowledgment. P.W. gratefully acknowledges the financial support of this research by the National Science of Foundation of China (NSFC) (No. 50103003), the "Qimingxing" Project (No. 01QE14011) of Shanghai Municipal Science and Technology Commission, and the "Shuguang" Project (No. 01SG05) of the Shanghai Municipal Education Commission and Shanghai Education Development Foundation.

References and Notes

(1) Aronhime, M. T.; Gillham, J. K. *J. Appl. Polym. Sci.* **1986**, *32*, 3589.
(2) Lucas, J. P.; Zhou, J. M. *Macromol. Compos. Sci. Technol.* **1995**, *53*, 57.
(3) Zhou, J. M.; Lucas, J. P. *Polymer* **1999**, *40*, 5505.
(4) Núñez, L.; Villanueva, M.; Fraga, F.; Núñez, M. R. *J. Appl. Polym. Sci.* **1999**, *74*, 353.
(5) Xiao, G. Z.; Shanahan, M. E. R. *J. Polym. Sci., Part B: Polym. Phys.* **1997**, *35*, 2659.
(6) Xiao, G. Z.; Shanahan, M. E. R. *J. Appl. Polym. Sci.* **1997**, *65*, 449.
(7) Guptu, V. B.; Drzal, L. T. *J. Appl. Polym. Sci.* **1985**, *30*, 4467.
(8) Aronhime, M. T.; Gillham, J. K. *J. Appl. Polym. Sci.* **1986**, *48*, 3589.
(9) Enns, J. B.; Gillham, J. K. *J. Appl. Polym. Sci.* **1983**, *28*, 2831.
(10) Johncock, P.; Tudgey, G. T. *Br. Polym. J.* **1986**, *18*, 292.
(11) Bellenger, V.; Verdue, J. *J. Mater. Sci.* **1989**, *24*, 63.
(12) Woo, M.; Piggott, M. *J. Compos. Technol. Res.* **198**7, *9*, 101.
(13) Adamson, M. *J. Mater. Sci.* **1980**, *15*, 1736.
(14) Apicella, A.; Nicolais, L.; De cataldis, C. *J. Membr. Sci.* **1985**, *18*, 211.
(15) Moy, P.; Karasz, F. E. *Polym. Eng. Sci.* **1980**, *20*, 315.
(16) Ding, Y. F.; Liu, M. J.; Li, S. J.; Zhang, S. Y.; Zhou, W. F. *Macromol. Chem. Phys.* **2001**, *202*, 2681.
(17) Ding, Y. F.; Li, H.; Liu, M. J.; Wu, X. G.; Li, S. J. *Chem. J. Chin. Univ.*, in press.
(18) Van alsten, J. G.; Coburn, J. C. *Macromolecules* **1994**, *27*, 3476.
(19) Sutander, P.; Ahn, D. J.; Franses, E. I. *Macromolecules* **1994**, *27*, 7316; *Thin Solid Films* **1995**, *263*, 134.
(20) Kusanagi, H.; Yukawa, S. *Polymer* **1994**, *35*, 5637.
(21) Murphy, D.; Dephinho, M. N. *J. Membr. Sci.* **1995**, *106*, 245.
(22) Macia, R.; Jack, Y. *J Chem. Soc.* **1996**, *92*, 2731.
(23) Fieldson, G. T.; Barbari, T. A. *Polymer* **1993**, *34*, 1193.
(24) Marechal, Y.; Chamel, A. *J. Phys. Chem.* **1996**, *100*, 8551; *Faraday Discuss.* **1996**, *103*, 349.
(25) Cotugno, S.; Larobina, D. *Polymer* **2001**, *42*, 6431.
(26) Noda. I. *Appl. Spectrosc.* **1993**, *47*, 1329.
(27) Noda. I. *Buil. Am. Phys. Soc.* **1986**, *31*, 520.
(28) Noda. I. *J. Am. Chem. Soc.* **1989**, *111*, 8116.
(29) Noda. I. *Appl. Spectrosc.* **1990**, *44*, 550.

(30) Czarnecki, M. A.; Wu, P.; Siesler, W. H. *Chem. Phys. Lett.* **1998**, *283*, 326.
(31) Liu, Y.; Ozaki, Y.; Noda, I. *J. Phys. Chem.* **1996**, *100*, 7327.
(32) Ozaki, Y.; Liu, Y.; Noda, I. *Macromolecules* **1997**, *30*, 2391.
(33) Czarnecki, M. A.; Maeda, H.; Ozaki, Y.; Suzuki, M.; Iwahashi, M. *J. Phys. Chem. A* **1998**, *102*, 6655.
(34) Ren, Y.; Shimoyama, K.; Ninomiya, T.; Matsukawa, K.; Inoue, H.; Noda, I.; Ozaki, Y. *Appl. Spectrosc.* **1999**, *53*, 919.
(35) Harric, N. J. *International Reflection Spectroscopy*; John Wiley: New York, 1967.

MA011819F